Applied Surface Science 258 (2011) 955–961

Contents lists available at SciVerse ScienceDirect

Applied Surface Science

journal homepage: www.elsevier.com/locate/apsusc

Effect of drying technique on the physicochemical properties of sodium silicate-based mesoporous precipitated silica

Pradip B. Sarawade[a], Jong-Kil Kim[b], Askwar Hilonga[a], Dang Viet Quang[a], Hee Taik Kim[a,*]

[a] Department of Chemical Engineering, Hanyang University, 1271 Sa 3-dong, Sangnok-gu, Ansan-si, Gyeonggi-do 426-791, Republic of Korea
[b] E&B Nanotech. Co., Ltd., Ansan-si, Republic of Korea

ARTICLE INFO

Article history:
Received 1 July 2011
Received in revised form 8 September 2011
Accepted 9 September 2011
Available online 14 September 2011

Keywords:
Mesoporous silica
Sodium silicate
Cost-effective
Microwave drying
Surface area

ABSTRACT

The conventional drying (oven drying) method used for the preparation of precipitated mesoporous silica with low surface area (>300 m^2/g) and small pore volume is often associated with a high production cost and a time consuming process. Therefore, the main goal of this study was to develop a cost-effective and fast drying process for the production of precipitated mesoporous silica using inexpensive industrial grade sodium silicate and spray drying of the precipitated wet-gel silica slurry. The precipitated wet-gel silica slurry was prepared from an aqueous sodium silicate solution through the drop-wise addition of sulfuric acid. Mesoporous precipitated silica powder was prepared by drying the wet-gel slurry with different drying techniques. The effects of the oven drying (OD), microwave drying (MD), and spray drying (SD) techniques on the physical (oil, water absorption, and tapping density), and textural properties (specific BET surface area, pore volume, pore size, and % porosity) of the precipitated mesoporous silica powder were studied. The dried precipitated mesoporous silica powders were characterized with field-emission scanning electron microscopy; Brunauer, Emmett and Teller and BJH nitrogen gas adsorption/desorption methods; Fourier-transform infrared spectroscopy; thermogravimetric and differential analysis; N_2 physisorption isotherm; pore size distribution and particle size analysis. There was a significant effect of drying technique on the textural properties, such as specific surface area, pore size distribution and cumulative pore volume of the mesoporous silica powder. Additionally, the effect of the microwave-drying period on the physicochemical properties of the precipitated mesoporous silica powder was investigated and discussed.

© 2011 Elsevier B.V. All rights reserved.

1. Introduction

Mesoporous precipitated silicas are good fillers of plastomers and elastomers. Precipitated silica compositions with polymers contribute to improvement of the tensile strength of the polymer–silica. Moreover, mesoporous precipitated silicas with high surface area and large pore volume are used as dielectric materials, elastomeric materials (such as tires), in flat panel displays, sensors, filters for exhaust gases and automobile exhaust systems, industrial pollutants, adsorbents, separations, biomedicine, sensors, drug delivery systems, oil-spill clean-up [1–5], and heterogeneous catalysts in various chemical reactions [6]. Generally, alkyl orthosilicates are used as a source of silica for the preparation of mesoporous silica. However, they are not the best commercial sources of silica due to their high cost, flammability, and difficulties in handling/storage. Therefore, their replacement with a comparatively less expensive and robust inorganic silica source is desired [7]. Sodium silicate (water-glass) could be a good source of silica for industrial, large-scale production of mesoporous silica powders.

We previously reported the preparation of hydrophobic mesoporous silica powder with high surface area and large pore volume via the surface modification of a wet-gel silica slurry [8]. Even though the mesoporous silica obtained through this method has excellent physical and textural properties, it is generally hydrophobic. These products thus have limited applications in various fields, such as moisture adsorption (desiccants). As a result, current efforts have been made to synthesize hydrophilic mesoporous precipitated silica powder with high specific surface area and large pore volume. For the synthesis of mesoporous silica powder, drying techniques are as important as the preparative parameters. Several researchers have investigated the effect of sol–gel preparative conditions on the synthesis of mesoporous silica powder. To the best of our knowledge, few reports have investigated the effects of drying technique on the morphology of silica powder. Rahman et al. reported some effects of drying technique on the morphology of nanoparticles synthesized via a sol–gel process; however, the authors used expensive silica alkoxides, such as tetraethoxysilane (TEOS) [9]. In addition, they did not report on the effects of the

* Corresponding author. Tel.: +82 31 400 5493; fax: +82 31 500 3579.
E-mail address: khtaik@yahoo.com (H.T. Kim).

0169-4332/$ – see front matter © 2011 Elsevier B.V. All rights reserved.
doi:10.1016/j.apsusc.2011.09.035

spray drying technique, which is very important for the industrial large-scale production of mesoporous precipitated silica powders using inexpensive sodium silicate solution. Considering the large-scale industrial production of mesoporous silica powder, there is a great need for the detailed investigation of the effects of the spray drying technique on the physicochemical properties of precipitated mesoporous silica powder.

In this study, oven drying (OD), microwave drying (MD), and spray drying (SD) techniques were used to dry a sodium silicate-based wet-gel silica slurry. The applied heating mechanism differentiates the spray drying technique from the conventional OD and MD methods. In the conventional OD method, the heat energy is transferred to the interior of the gel/slurry via conduction. The heat conduction rate depends on the thermal conductivity of the wet-gel silica slurry and decreases significantly as the moisture content in the gel decreases, thereby prolonging the drying process [10–12]. Whereas, in the MD process, water present in the gel/slurry absorbs the microwaves throughout the entire mass, causing molecular vibrations with respect to the oscillating electric field of the microwaves and thus uniformly heating the gel/slurry [13]. In the SD process, the size-controlled drops of the liquid or slurry are dispersed through the nozzle into a hot air chamber. Liquid (water) in the wet-gel slurry absorbs the hot air, facilitating the uniform heating of the entire mass. Ultimately, this accelerates the drying process and reduces the total drying time as well as the production cost. This drying process is a rapid one-step process that eliminates the need for additional processing and is therefore suitable for large-scale industrial production of mesoporous silica powders. Therefore, the macroscopic drying phenomena of various drying techniques have significant effects on the textural properties (BET specific surface area, pore size, cumulative pore volume, and % porosity) of mesoporous silica powder. Our findings should be applicable to the large-scale industrial mass-production of hydrophilic, precipitated mesoporous silica powders with improved properties.

2. Experimental

2.1. Materials

An industrial-grade sodium silicate solution (water-glass molar ratio $SiO_2/Na_2O = 3.4$; density 1.280 g/cm^3) as a silica precursor was purchased from Shinwoo Materials Co. Ltd., NaCl (99.5%) from Showa Chemical Co., Ltd., and sulfuric acid (98%) from Duksan Pure Chemicals Co., Ltd. All reagents were used without further purification.

2.2. Preparation of a wet-gel silica slurry through the drop-wise addition of sulfuric acid into an aqueous sodium silicate solution

Silica wet-gel slurry was prepared from an aqueous sodium silicate solution through the addition of sulfuric acid using the precipitation method under constant stirring. Initially, 2080 g of a 24% sodium silicate solution ($Na_2O{\cdot}SiO_2$) was added to 6682 g of aqueous NaCl (4%) in a 10 L reactor tank. The temperature was adjusted to 35 °C under constant stirring at a speed of 300 rpm. The 8% H_2SO_4 was added to the alkaline solution in two steps. In the first step, 985 g of 8% H_2SO_4 was added to the mixture by a chemical feed pump at a rate of 197 g/min; the semi-gelatic point was achieved within a minute. In order to prevent the formation of a strong silica gel, the solution was stirred for an additional 10 min with no further addition of H_2SO_4. The second step involved the addition of more 8% H_2SO_4 (1580 g) until the pH of the silica slurry reached 5. After the final addition of 8% H_2SO_4, the precipitated wet-gel silica slurry was aged for an hour at 85 °C under constant stirring (150 rpm) and then cooled to room temperature. The prepared wet-gel silica slurry was thoroughly washed to remove by-products (Na^+, Cl^-, SO_4^{2-}) and filtered using a filter press (laboratory scale to obtain a wet-cake). The removal of Na^+ from the washed cake was confirmed using a sodium ion detector (NeoMet, ISTEK, pH/ISE meter). Furthermore, the washed cake was dried using different drying techniques (oven drying, microwave drying, and spray drying).

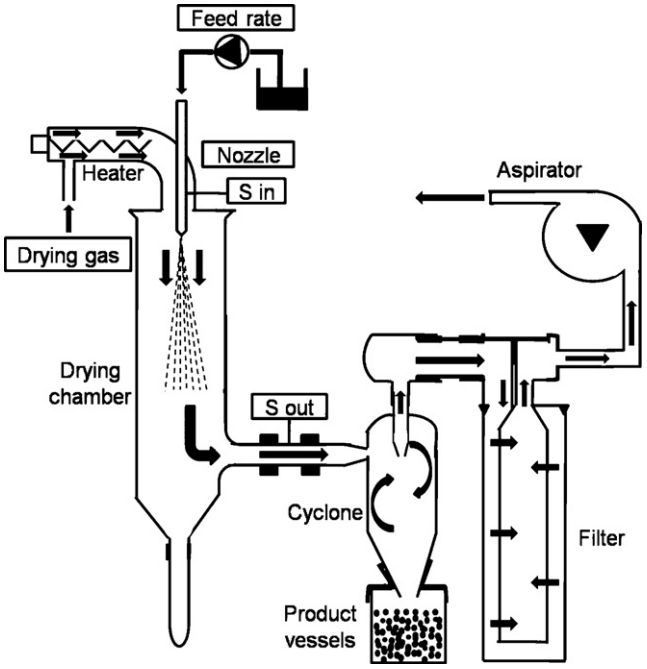

Scheme 1. Schematic diagram of the spray drying process.

2.3. Drying of washed cake with different drying techniques

2.3.1. Oven drying

The obtained wet-cake was directly dried at 80 °C for 4 h in an oven. To complete remove water, the cake was dried at 200 °C for an hour. The dried cake was crushed into a powder for characterization.

2.3.2. Microwave drying

The wet-cake was dried at an ambient pressure in a microwave oven (operating frequency of 2.45 GHZ, 0.7 kW). The time interval between successive microwave exposures and the total drying time varied from 10 to 30 min.

2.3.3. Spray drying

The spray-dry instrument used in this study was a pilot plant apparatus made by E & B Nanotech Co. Ltd., Korea. Droplets were generated from a single-flow spray nozzle, and the nozzle pressure was varied from 0.05 to 0.30 MPa. The temperatures, which were controlled from 100 to 180 °C, were digitally displayed. The cyclone collector used to collect the spray-dried samples employed centrifugal force created by a circular flow that accelerated the particles toward the cyclone wall, as shown in Scheme 1. The wet-cake was dried using a spray-drying technique. For this purpose, the 1000 g wet-cake was mixed with 500 g water (50%), continuously stirred and fed into the spray-drier with a peristaltic pump that operated at a speed of 100 rpm. The liquid was atomized at 10 kPa in a nozzle using an airflow rate of 75 m^2/min. The spray-dryer outlet and inlet temperatures were maintained at 100 and 180 °C, respectively. These processing conditions were maintained throughout the drying process. The total drying period for a 1500 g

Table 1
Effects of drying technique on the physical and textural properties of precipitated mesoporous silica powder.

No.	Drying technique	Surface area (m^2/g) BJH method	Taping density (g/cm^3)	Pore diameter (nm)	Pore volume (cm^3/g) BJH method	Porosity (%)	Water absorption (ml/g)	Oil absorption (ml/g)	Moisture contents (%)
1	Oven drying	358	0.362	7.51	0.91	80.95	2.38	2.19	5.62
2	Microwave drying	437	0.294	10.21	1.27	84.52	2.86	2.34	4.46
3	Spray drying	679	0.225	17.41	1.96	88.16	3.79	3.51	2.17

slurry was 15 min. Spray drying was a one-step rapid procedure that eliminated additional processing, and the present route is a suitable alternative for large-scale industrial production.

2.4. Characterization methods

The effects of different drying techniques on the textural properties of the precipitated mesoporous silica powders (packing density, porosity, oil absorption, and water absorption) were measured using previously described methods [14]. For the water absorption test of the dried silica samples, 10 g of dried silica powder was placed on polyethylene, which did not absorb water. Water was added drop-wise to the center of the powder, and the mixture was thoroughly kneaded with a spatula after each addition. The dropping and kneading were repeated until the entire sample became a solid lump of putty. The amount of water added was recorded, and the water absorption was expressed in terms of ml/g (volume of water absorbed/weight of the sample).

For the oil absorption test of the silica samples, dioctyl phthalate (DOP) was used. The procedure used for the oil absorption test was similar to that used for the water absorption test. The amount of oil absorption was expressed in terms of ml/g (volume of oil absorbed/weight of the sample). The moisture contents of the silica samples dried with different drying techniques were determined using an infrared moisture determination balance (Model Kett 610, AC100-240 50/60 Hz, Japan). A 5 g silica sample was placed in a weigh pan and held for 30 min. The tapping density of mesoporous silica powder was determined by filling a cylindrical column of known volume with silica powder; densities were then calculated by comparing the mass of the silica powder to the volume ratio. Calculations were performed in triplicate for each sample, and the average was recorded as the tapping density of the silica powder.

The specific surface area, average pore size, cumulative pore volume, N_2 gas adsorption/desorption isotherms, and pore size distributions (PSDs) of dried silica powders were characterized by a BET N_2 gas adsorption/desorption (77 K) apparatus (ASAP 200, Micromeritics, USA). The samples were degassed at 200 °C for 2 h under vacuum (10^{-3} mmHg). The BJH method and desorption isotherm data were used to calculate the total pore volume and pore size distributions, respectively [15]. A Perkin-Elmer 2000 FTIR spectrometer was employed to observe the drying technique effects on the intensities of the silica surface hydroxyl groups (–OH). For this purpose, silica powders were mixed with KBr and pressed to form a sample pellet for FTIR measurements. Samples were examined by TG-DTA to study the drying technique effects on the mesoporous silica. Ten milligrams of the mesoporous silica powder was heat-treated in air from room temperature (25 °C) to 1000 °C at a controlled heating rate of 1.5 °C min^{-1} using a microprocessor-based Parr temperature controller (Model 4846) connected to a muffle furnace (A.H. JEON Industrial Co., Ltd., Korea).

Microstructural studies of the mesoporous silica powders were performed using a field-emission scanning electron microscope (FE-SEM, Hitachi, S-4800) and X-ray energy dispersive spectroscopy (EDS). EDS was also employed to examine the purity of the final product. A transmission electron microscope (TEM, JEOL JSM 6700 F) was used to analyze the morphologies of the mesoporous silica powders at an accelerating voltage of 80 kV. The dried samples (oven drying, microwave drying, and spray drying) were dispersed in water and placed on copper grids covered with a carbon coating for TEM observation.

The errors in the % porosity, packing density, water absorption and oil absorption measurements were calculated as a root mean square (RMS) using the formula $[\sum\{x-x^-\}^2/4]^{1/2}$, where x and x^- represent the actual and mean values, respectively. The results reported in this study were based on the average of three sets of experiments.

3. Results and discussion

3.1. Effects of drying technique on the physical properties of the precipitated mesoporous silica powder

The amounts of water and oil absorbed by the precipitated mesoporous silica powder were measured to evaluate the effects of the drying techniques on the physical properties of the mesoporous silica powder. The amounts of water and oil absorption for dried mesoporous silica powders prepared using the different drying techniques are compared in Table 1. Whereas, the effects of the microwave-drying period on the physicochemical properties of the precipitated mesoporous silica powder are compared in Table 2. The silica samples dried by the SD technique (3.79 ml/g) absorbed more water than the samples dried by the OD technique (2.38 ml/g). Additionally, SD mesoporous silica samples had very high oil absorption capacities compared to the samples dried by the OD method. The MD samples absorbed more oil than the samples dried by OD and less than the SD samples. The tapping densities of precipitated mesoporous silica samples dried by oven, microwave, and spray drying techniques are summarized in Table 1. The tapping density value obtained for mesoporous silica powder dried by the SD process was less than the tapping density obtained for the samples dried by the OD technique. However, the tapping density obtained for the samples dried by the MD technique was less

Table 2
Effects of microwave-drying period on the physicochemical (physical and textural) properties of precipitated mesoporous silica powder.

No.	Microwave-drying period (min.)	Surface area (m^2/g) BET method	Taping density (g/cm^3)	Pore diameter (nm)	Pore volume (cm^3/g) BJH method	Porosity (%)	Water absorption (ml/g)	Oil absorption (ml/g)	Moisture contents (%)
1	10	426	0.281	10.06	1.21	84.41	2.73	2.23	4.95
2	20	432	0.287	10.13	1.23	84.46	2.79	2.29	4.58
3	30	437	0.294	10.21	1.27	84.52	2.86	2.34	4.41

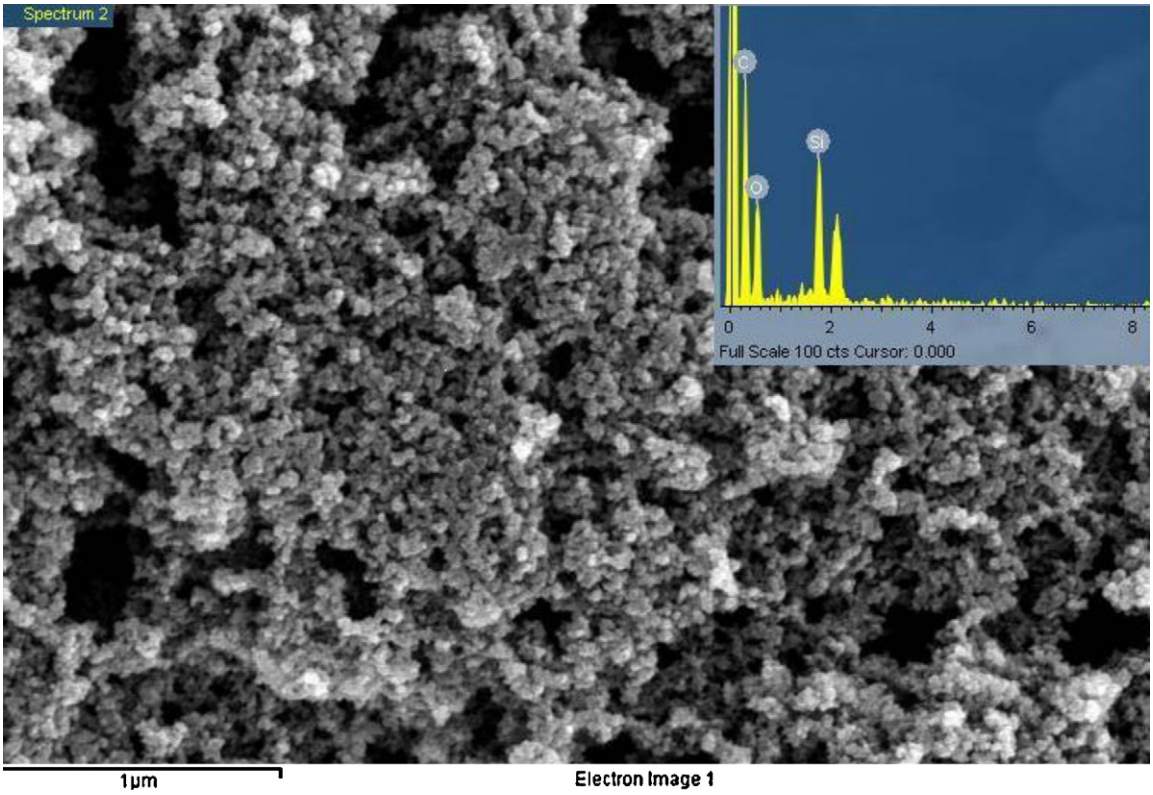

Fig. 1. EDS spectra of the sodium silicate-based precipitated mesoporous silica powder.

than those of the SD technique, which indicates that SD could preserve the porous structure and hence the porosity. In the OD technique, high shrinkage could be obtained for the wet-gel silica slurry, hence an increase in the drying shrinkage density increased for the mesoporous silica sample dried by the OD technique. Alternatively, relatively less drying shrinkage occurred due to uniform heating of the wet-gel silica slurry droplet in the hot chamber. Hence, due to the decrease in drying shrinkage, the tapping density of the mesoporous silica powder decreased for the spray dried silica sample.

Fig. 1 demonstrates the purity of the obtained mesoporous silica powder dried with the SD technique. Fig. 1 shows that only the expected EDS peaks for Si, O, and C were observed, emphasizing the purity of the obtained mesoporous precipitated silica product.

3.2. *Effects of drying technique on the textural properties of the precipitated mesoporous silica powder*

The textural properties (specific surface area, cumulative pore volume, pore size, and % porosity) of mesoporous silica powders prepared with various drying techniques are compared in Table 1. The largest BET specific surface area was obtained for the SD technique, and a lower value was obtained for the OD technique. A relatively lower BET surface area was obtained for the MD technique. Additionally, the cumulative pore volume and average pore diameters obtained for the spray-dried sample were much greater than the samples dried by OD and MD techniques. This can be attributed to less drying shrinkage during the SD technique due to uniform heating of the wet-gel silica slurry drops in the hot chamber [14]. In contrast, the drying shrinkage occurring in the OD and MD techniques could be relatively high. Hence, the drying shrinkage can reduce the total pore volume and pore size (pore diameter). Therefore, decreases in the total pore volume (reduction in microporous area) and BET specific surface area are reduced in the case of oven-dried samples. The spray-dried sample had a comparatively low tapping density compared to those of the oven- and microwave-dried samples, hence the % porosity calculated for the spray-dried sample was very high. The moisture content observed for the spray-dried sample was relatively less than those of the sample dried by the OD and MD techniques. The water contents of the samples produced from MD and OD techniques was 4.46 and 5.62%, respectively, indicating that the SD technique effectively removed water molecules in less time and at a lower temperature than could be achieved in the OD or MD techniques.

3.3. *Nitrogen physisorption studies*

N_2 adsorption and desorption isotherms and the pore size distribution of the mesoporous silica powders were studied to determine the effect of drying technique on the nature of the pores in the mesoporous silica network. Fig. 2 shows the N_2 adsorption/desorption isotherms of OD, MD and SD silica samples. All samples showed similar isotherms and were comparable to mesoporous materials (H1 type) [16,17], although differences in surface area, pore volume, and pore size were observed. H1-type hysteresis loops indicated cylindrical pores [18], and large hysteresis loops indicated more pores in the silica network. The physisorption isotherms obtained for all silica samples exhibited similar hysteresis loops, which correspond to characteristic features of mesoporous materials (type IV isotherms) [19,20].

The absorption volumes of each silica sample differed based on the drying technique. The maximum amount of N_2 gas adsorbed by a porous solid obviously depends on the volume of the pores present in the porous material [21]. Spray-dried mesoporous silica powders absorbed more than did the OD and MD mesoporous silica samples. In the SD process, size-controlled drops of wet-gel silica slurry were dispersed by a nozzle into the hot air chamber. The liquid (water) present throughout the wet-gel silica slurry uni-

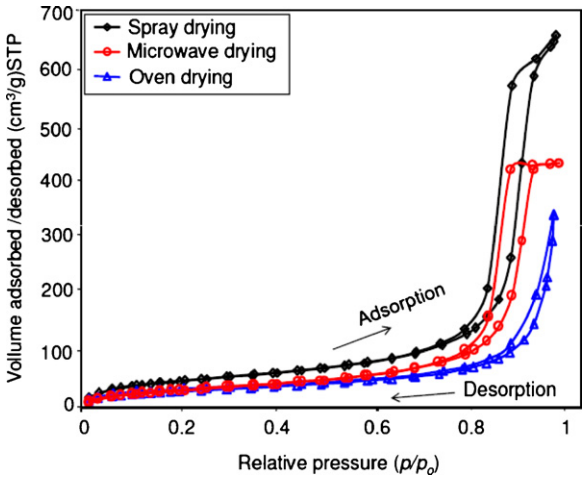

Fig. 2. N_2 adsorption/desorption isotherms of the precipitated mesoporous silica powders prepared using different drying techniques (N_2 adsorption/desorption data were calculated by BJH method).

formly absorbed the hot air, facilitating uniform heating of the mass dispersed through the nozzle, which may have reduced the drying shrinkage of the mesoporous silica. Ultimately, this increased the total pore volume and the porosity [14]. In the case of the OD process, the water molecules were constantly eliminated from the pores, causing an increase in the capillary force, thereby increasing the drying shrinkage. Hence, the increase in drying shrinkage due to meso/micropores in the silica network was reduced, which caused decreases in the pore diameter, total pore volume, and % porosity.

Fig. 3 shows the pore size distribution (PSDs) curves of mesoporous silica powders obtained by OD, MD and SD techniques. The OD mesoporous silica sample had a narrow pore size distribution with an average pore diameter of 7.51 nm. The MD mesoporous silica powder had a broad pore size distribution with an average peak pore diameter of 10.21 nm, while SD mesoporous silica powder had a broader pore size distribution with an average diameter of 17.41 nm. As shown in Fig. 3(c), the peak pore diameter for the SD silica sample shifted toward a higher value. All of the drying techniques reported in this study showed a pronounced peak in the mesopore region (2–50 nm) [22], indicating that the silica samples maintained mesoporosity even after drying.

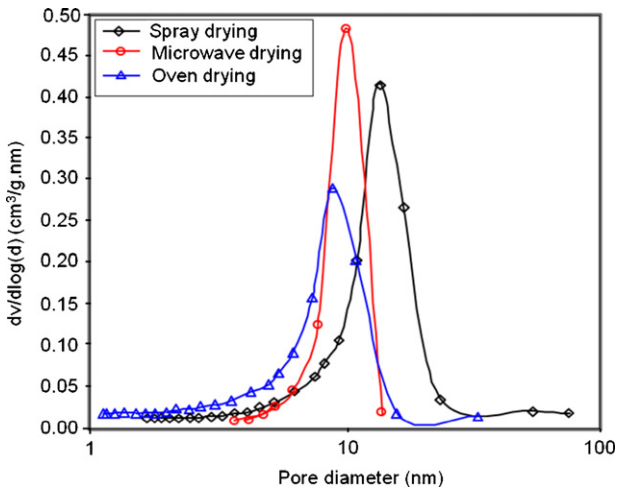

Fig. 3. Cumulative pore size distributions of the mesoporous silica powders prepared by oven, microwave, and spray drying techniques (pore size distribution data were calculated by BJH method).

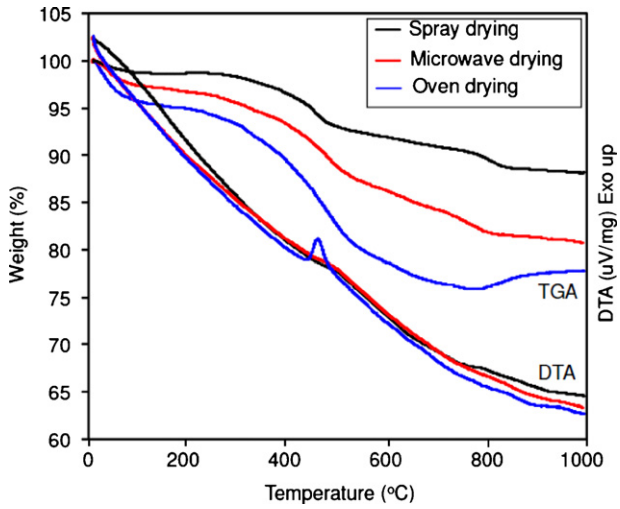

Fig. 4. TG/DTA curves of hydrophilic mesoporous silica powders prepared using different drying techniques.

3.4. TG-DTA and FTIR studies of the precipitated mesoporous silica powder

The effects of drying technique on the thermal stability of the sodium silicate-based precipitated mesoporous silica powders were studied using TG-DTA analysis. Fig. 4(a–c) shows the TG-DTA analysis results of the precipitated mesoporous silica powders dried by sprayed, MD and SD techniques. The initial weight loss observed for all samples up to 160 °C was due to the evaporation of the residual water molecules (remaining moisture) from the precipitated mesoporous silica powder. As observed from the TG curve, the initial weight loss observed for the SD silica sample was comparatively less than those of the OD and MD silica samples, which indicates that the SD technique can more effectively remove moisture from the wet-gel silica slurry. Furthermore, OD and MD techniques show more weight loss with an increase in temperature to greater than 430 °C. As observed from the DTA curve, there was not much difference between the silica samples. The DTA curves obtained for precipitated mesoporous silica samples dried by the OD, MD and SD techniques were quite similar.

The effects of drying technique on chemical bonding in the sodium silicate-based mesoporous silica powders were studied using FTIR spectroscopy. FTIR spectra of the silica samples dried by OD, MD and SD techniques are shown in Fig. 5. The peaks centered at 1070 and 495 cm^{-1} correspond to the Si–O–Si bonds and

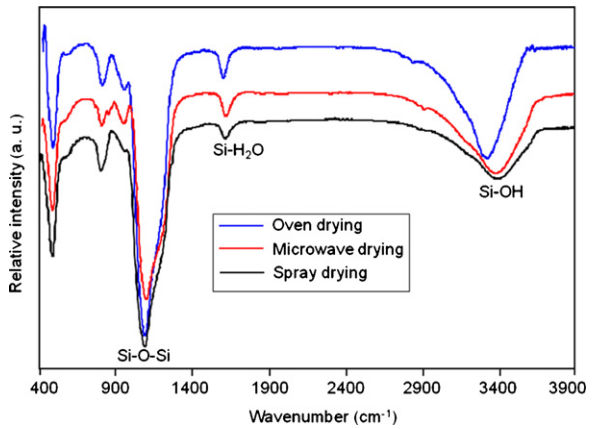

Fig. 5. FTIR spectra of the precipitated mesoporous silica powders prepared by oven, microwave, and spray drying techniques.

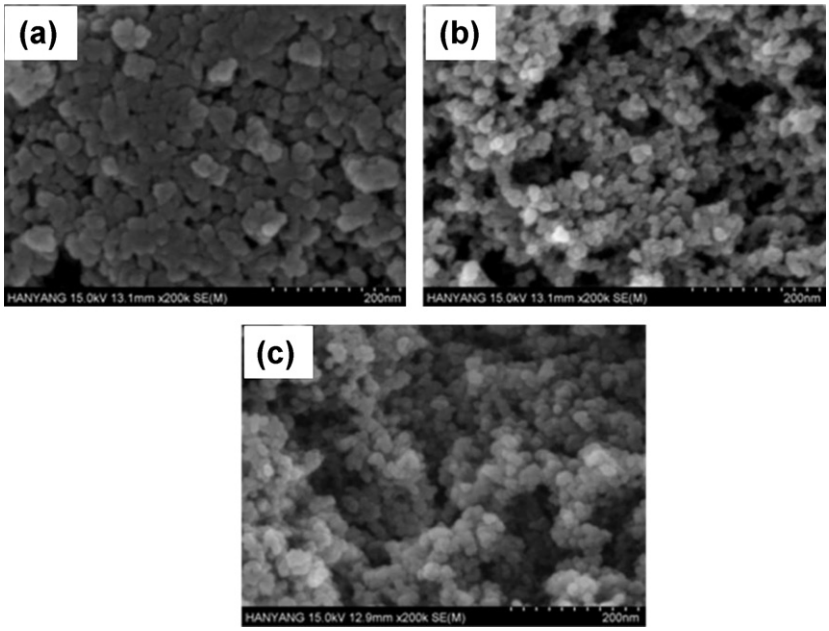

Fig. 6. FE-SEM micrograph of the mesoporous silica powders prepared using different drying techniques (a) oven drying (b) microwave drying, and (c) spray drying.

were the most informative of the silica network structure [23,24]. The broad absorption peak centered at 3390 cm^{-1} was attributed to the O–H stretching band of hydrogen-bonded water molecules (H–O–H···H_2O). The strong absorption peaks at 3390 cm^{-1} and 1640 cm^{-1} correspond to the terminal–OH groups. The strong absorption peaks observed at 3390 cm^{-1} and 1640 cm^{-1} were comparatively less intense (stretched) for the samples dried by the SD technique [7]. This indicates that the SD technique was more effective in removing the water molecules from the sodium silicate-based precipitated wet-gel silica slurry. The FTIR results are also supported by the results of TGA and moisture absorption tests (Table 1), as previously discussed. In contrast, for the OD silica powder, a strong–OH peak (less stretched) at 3390 cm^{-1}, indicated that a significant fraction of the Si atoms existed on the surface of the silica network structure as hydroxylated species [9]. This confirmed the efficiency of the SD technique in removing water from the precipitated wet-gel silica slurry.

3.5. *Effects of drying technique on the nanostructure of precipitated mesoporous silica powder*

The effects of different drying techniques on the mesoporous structure of silica powders were observed using FE-SEM. Fig. 6 shows the pore characteristics and structural morphology of precipitated mesoporous silica based on FE-SEM micrographs of (a) OD (b) MD and (c) SD mesoporous silica powders. Generally, the OD silica powder was characterized by dense aggregates of larger spheres (consisting of closely packed particles) with a smaller pore size (Fig. 6(a)) [9]. This can be attributed to the OD process in which the water molecules were constantly eliminated, causing an increase

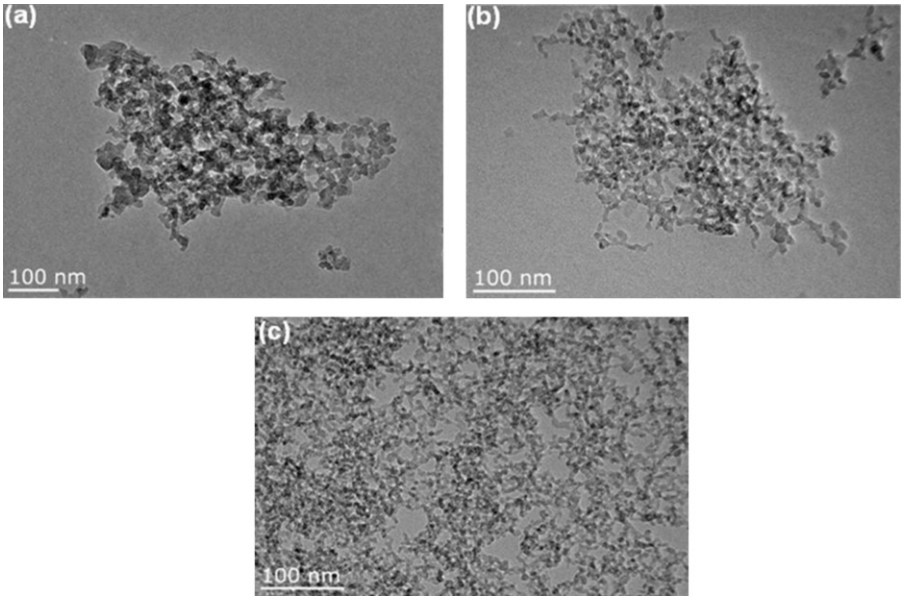

Fig. 7. TEM micrograph of the mesoporous silica powders prepared using different drying techniques (a) oven drying (b) microwave drying, and (c) spray drying.

in silica sol concentration and creating fluid drag, which forced the particles closer to each other. At a critical point of drying, these particles touch and form an aggregate to achieve greater stability. Hydrogen bonding (through silanol groups), van der Waals and capillary forces were dominant attraction forces acting on these nanoparticles [25,26].

The MD silica powder had a more porous structure with smaller particle size and larger pore size (Fig. 6(b)). The precipitated mesoporous silica prepared by the SD technique appeared to have particles that were small and uniform in size. The pore size for the spray-dried silica sample was more broadly distributed than those of the OD and MD silica samples. Fig. 7 shows representative TEM micrographs of (a) OD (b) MD and (c) SD precipitated mesoporous silica powders. Oven- and microwave-dried precipitated silica powders showed less porous silica network microstructures with irregular pore sizes. Alternatively, the sample prepared with the SD technique exhibited a highly porous, sponge-like silica microstructure with a uniform pore size distribution in the range of 12–18 nm. The wet-gel silica slurry experienced less shrinkage during spray drying as it uniformly absorbed the hot air, facilitating uniform heating of the entire mass dispersed through the nozzle, leading to the formation of highly porous, dried silica powder microstructures. The surface morphology of the SD mesoporous silica structure observed by TEM was more uniform and had a relatively smaller particle size than did the OD silica sample.

4. Conclusions

In the present study, we studied the effects of different drying techniques (oven, microwave, and spray) on the physical (taping density, oil absorption, and water absorption), textural properties (specific BET surface area, pore volume, pore size, and % porosity), and morphology of precipitated mesoporous silica synthesized by sol–gel polymerization of a sodium silicate solution. The drying technique had strong effects on the properties of the final product due to its great impact on the precipitated wet-gel silica slurry, primarily on the tapping density, oil/water absorption, surface area, pore volume, pore diameter, % porosity, and morphology. The precipitated silica obtained by the SD technique exhibited a highly porous, sponge-like mesoporous nanostructure with uniform particle and pore size distribution. The SD precipitated mesoporous silica had superior properties of high surface area (679 cm^2/g), low tapping density (0.225 g/cm^3), large pore diameter (17.41 nm) and large cumulative pore volume (1.96 cm^3/g). The SD technique effectively removed the water from the wet-gel silica slurry synthesized via sol–gel polymerization of sodium silicate (water-glass). Spray drying is proposed as the best drying technique for the large-scale industrial mass production of highly porous (high BET surface area, large pore volume and pore diameter) silica powders.

Acknowledgment

This work was supported by the research fund of Hanyang University (HY-2011-N).

References

[1] G.M. Pajnok, Appl. Catal. 72 (1991) 21.
[2] A.S. Dias, M. Pillinger, A.A. Valente, Microporous Mesoporous Mater. 94 (1–3) (2006) 214.
[3] M.R. Jamali, Y. Aassadi, F. Shemirani, M.R.M. Hosseini, R.R. Kozani, M.M. Farahani, M.S. Niasani, Anal. Chem. Acta 579 (1) (2006) 68.
[4] A.V. Rao, N.D. Hegde, H. Hirashima, J. Colloid Interface Sci. 305 (1) (2007) 124.
[5] Q. Tang, Y. Xu, D. Wu, Y. Sun, J. Solid State Chem. 179 (5) (2006) 1513.
[6] M.J. Lee, J.Y. Kim, Sci. Technol. Ceram. Mater. 7 (4) (1992) 429.
[7] P.B. Sarawade, J.K. Kim, J.K. Park, H.K. Kim, Aerosol Air Qual. Res. 6 (1) (2006) 105.
[8] P.B. Sarawade, J.K. Kim, A. Hilonga, H.T. Kim, Powder Technol. 197 (2010) 288.
[9] I.A. Rahman, P. Veayakumaran, C.S. Spaut, J. Ismail, C.K. Chee, Ceram. Int. 34 (2008) 2059.
[10] C.J. Brinker, G.W. Scherer, Sol–Gel Science, Academic Press, San Diego, 1990, p. 662.
[11] S.D. Bhagat, K.T. Park, Y.H. Kim, J.S. Kim, J.H. Han, Solid State Sci. 10 (9) (2008) 1113.
[12] H.S. Yang, S.Y. Choi, S.H. Hyun, H.H. Park, J. Non–Cryst. Solids 221 (1997) 151.
[13] S.D. Bhagat, Y.H. Kim, K.H. Suh, Y.S. Ahn, J.G. Yeo, J.H. Han, Microporous Mesoporous Mater. 112 (2008) 504.
[14] P.B. Sarawade, J.K. Kim, A. Hilonga, H.T. Kim, Solid State Sci. 12 (2010) 911.
[15] G. Reichenauer, G.W. Scherer, J. Colloid Interface Sci. 236 (2001) 385.
[16] D.J. Suh, T.J. Park, J.H. Sonn, J.C. Lim, J. Mater. Sci. Lett. 18 (1999) 1473.
[17] P.B. Sarawade, J.K. Kim, A. Hilonga, H.T. Kim, Korean J. Chem. Eng. 27 (4) (2010) 1301.
[18] G.T. Burns, Q. Deng, R. Field, J.M. Hahn, C.W. Lengtz, Chem. Mater. 11 (1999) 1275.
[19] A.C. Pierre, E. Elaloui, G.M. Pajonk, Langmuir 14 (1998) 66.
[20] W.C. Li, A.H. Lu, S.C. Guo, J. Colloid Interface Sci. 254 (2002) 153.
[21] P.B. Sarawade, J.K. Kim, A. Hilonga, D.V. Quang, H.T. Kim, Microporous Mesoporous Mater. 139 (2011) 138.
[22] K.S.W. Sing, D.H. Everett, R.A.W. Haul, L. Moscou, R.A. Pierotti, J. Rouquerol, T. Siemieniewska, Pure Appl. Chem. 57 (4) (1985) 603.
[23] R.A. Oweini, H.E. Rassy, J. Mol. Struct. 919 (2009) 140.
[24] C.J. Brinker, S.W. Scherere, Sol–Gel Science: The Physics and Chemistry of Sol–Gel Processing, Academic press, San Diego, 1990, p. 501.
[25] S. Kwon, G.L. Messing, Boehmite Nanostruct. Mater. 8 (1997) 399.
[26] C.J. Brinker, G.W. Scherer, Sol–Gel Science: The Physics and Chemistry of Sol–Gel Processing, Academic Press Inc., San Diego, 1990.